EXAFS Study of Refractory Cement Phases: CaAl2O14H20, Ca2Al2O13H16, and Ca3Al2O12H12

N. Richard, N. Lequeux, P. Boch

Classification
Physics Abstracts
07.85 — 32.20R — 78.70

EXAFS Study of Refractory Cement Phases: $CaAl_2O_{14}H_{20}$, $Ca_2Al_2O_{13}H_{16}$, and $Ca_3Al_2O_{12}H_{12}$

N. Richard, N. Lequeux and P. Boch

UA-CNRS Matériaux Inorganiques, Ecole Supérieure de Physique et de Chimie Industrielles de Paris, 10 rue Vauquelin, 75005 Paris, France

(Received 24 April 1995, accepted 19 June 1995)

Résumé. — La spectroscopie d'absorption des rayons X est utilisée pour la première fois pour caractériser l'environnement local autour de l'aluminium et du calcium dans des phases formées par hydratation de ciments alumineux. Le spectre EXAFS au seuil K du calcium confirme que C_2AH_8 est une phase AFm. De plus, on indique une position pour les cations aluminium de l'intercouche, qui sont dans un site tétraédrique hydraté. Les expériences d'absorption au seuil K de l'aluminium révèlent une analogie entre la structure de CAH_{10} et celle de la gibbsite AH_3. Le modèle structural proposé pour CAH_{10} est basé sur l'existence de deux anneaux formés chacun de six octaèdres $[Al(OH)_6]^{3-}$ liés par arêtes, les atomes de calcium assurant un lien entre ces anneaux. Les ciments alumineux sont couramment utilisés pour des applications réfractaires ; c'est pourquoi cette étude suit l'évolution de l'environnement autour du calcium et de l'aluminium au cours de la déshydratation de CAH_{10}. Une diminution progressive de la distance Ca-O, ainsi qu'une réduction du nombre de voisins oxygène dans la première couche de coordination autour du calcium sont mis en évidence lors de la déshydratation.

Abstract. — X-ray absorption spectroscopy (EXAFS and XANES) is used for the first time to characterize the local environment of aluminium and calcium in phases formed by hydration of high-alumina cements. Ca K-edge EXAFS spectrum confirms that C_2AH_8 is an AFm phase. A location is given for the interlayer aluminium cations, which are in a tetrahedrally coordinated hydrated site. Absorption measurements at the Al K-edge show a structural analogy between CAH_{10} and gibbsite AH_3. The structural model proposed for CAH_{10} is based on two rings of six edge-sharing $[Al(OH)_6]^{3-}$ octahedra, with Ca^{2+} cations linking them together. High-alumina cements are commonly used for refractory applications. Changes in aluminium and calcium environments during CAH_{10} dehydration is therefore investigated by X-ray absorption spectroscopy. Dehydration leads to a decrease in the Ca-O distance and reduces the number of oxygen neighbours in the first coordination shell around calcium.

Introduction

The cements that are used for making buildings are "Portland cements". Their main phases are located within the diagram $CaO\text{-}SiO_2\text{-}Al_2O_3\text{-}Fe_2O_3$. The cements that are used for making refractories are "high-alumina cements". They correspond to the diagram $CaO\text{-}Al_2O_3$ [1]. This study is devoted to high-alumina cements whose main constituents are calcium aluminates.

Hydration of cements results in the formation of one or more hydrates of which the more prominent phases are CAH_{10}, C_2AH_8, C_3AH_6, and gibbsite AH_3 (we use the standard notation for cement: C = CaO, A = Al_2O_3, H = H_2O). The nature of the hydrate(s) formed depends on the temperature of hydration [2]. Many doubts subsist regarding the structure of CAH_{10} and C_2AH_8; these have pseudohexagonal symmetry (probably monoclinic) and are formed at temperatures below 25 °C. Cubic C_3AH_6 and monoclinic AH_3 are the stable phases formed at $T > 50$ °C.

Dehydration of high-alumina cements is accompanied by stepwise removal of water. The dehydrated products of CAH_{10} and C_2AH_8 are amorphous, whilst dehydration of C_3AH_6 gives rise to crystallized products. The study of the dehydration behaviour of CAH_{10}, investigated in this paper, is important for at least two reasons. First, a major use of high-alumina cements is for making refractory concrete, and it is useful to understand what happens to the hydrates during the first stages of heating. Second, the phenomenon of conversion (transformation of CAH_{10} into C_3AH_6 and AH_3) is of practical importance because it can lead to a strong decrease in mechanical properties.

Most cementitious phases being badly crystallized, the knowledge of the short-range order is of prime importance. ^{27}Al and ^{29}Si Nuclear Magnetic Resonance (NMR) are useful for characterizing the environment of aluminium and silicon, respectively. For calcium, however, the use of ^{43}Ca NMR encounters the problem of the very low natural abondance of ^{43}Ca (0.145%).

In the present study, X-ray absorption spectroscopy is used for the first time to study the calcium aluminate phases formed by hydration of high-alumina cements. Results about Ca and Al K-edge X-ray Absorption Near-Edge Spectroscopy (XANES) and Extended X-ray Absorption Fine Structure (EXAFS) are reported for CAH_{10}, C_2AH_8 and C_3AH_6. Changes in the short-range order of CAH_{10} during heat treatments are also presented. Additional information obtained by ^{27}Al NMR and powder X-Ray Diffraction (XRD) is reported.

1. Experimental

1.1. Preparation and Characterization of Materials. — C_3AH_6 was obtained hydrothermally from tricalcium aluminate C_3A hydrated at 120 °C for 15 days.

C_2AH_8 was synthetized using a two-stage method: firstly, a solid reaction at 1450 °C between a mixture of CaO and α-Al_2O_3 with the stoechiometry C:A = 2:1 gave a mixture of C_3A and $C_{12}A_7$. Secondly, the mixture was rolled with excess distilled water for 48 h at room temperature. The hydrate C_2AH_8 formed was filtered and dried by washing it with acetone and ether. The exact composition of the hydrate was $C_2AH_{7.5}$. CAH_{10} was prepared by dissolving a Fondu cement (Lafarge, C:A = 1:1 in molar ratio) in distilled water and shaking for 90 min at 10 °C under a flux of nitrogen. After filtration, the liquor was kept 24 h at 5 °C in CO_2-free air; CAH_{10} precipitated and was filtered, then dried with the same procedure as described for C_2AH_8. The XRD powder pattern of CAH_{10} indicated traces of gibbsite AH_3. X-ray fluorescence confirmed the C/A ratio of 1. The water content deduced from TGA gave a formula of $CAH_{9.4}$ which could be due to a partial dehydration during storage at 4 °C.

The phase purity of all the phases was checked by powder XRD; X-ray measurements (Philips PW 1710) were performed with graphite monochromated CuKα radiation, with the following experimental conditions: step width of 0.02°, counting time of 30 s/step and a scanning range of $2\theta = 4°$ to 80°. Chemical analysis was performed by X-ray fluorescence. Infra-Red (IR) and DTA-TGA were also used to characterize the hydrates.

CAH_{10} was subjected to dehydration at a temperature T_0 for 24 hours, in a thermogravimetric apparatus in which the weight losses and the temperature were recorded. After the heat treatment, the resulting product was controlled by DTA-TGA and XRD.

1.2. X-Ray Absorption Spectroscopy

1.2.1. Experimental Set-up. — The experiments at the Ca K-edge (4038 eV) were performed at low temperature (20 K) at LURE (Orsay, France), using the DCI storage ring operating at 300 mA and 1.85 GeV. Monochromatization was achieved through a Si(111) double crystal monochromator. The Ca K-edge absorption spectra were recorded between 3950 and 4700 eV with steps of 1 eV (4 s/step) for the EXAFS measurement, and between 3975 and 4120 eV with steps of 0.3 eV (4 s/step) for XANES. Absorption was recorded in the transmission mode. Incident and transmitted intensities were measured with ionization chambers filled with helium and neon gas.

The Al K-edge (1559 eV) absorption measurements were performed on the LURE/SuperACO synchrotron radiation facility (Orsay, France); the ring operated at 800 MeV and 300 mA. Monochromatization was achieved through two α-quartz crystals cut along $(10\bar{1}0)$. Al K-edge XANES spectra were collected over a photon range of 1550-1600 eV using 0.2 eV steps (1 s/step); EXAFS was recorded between 1550 and 1800 eV by steps of 1 eV (1 s/step). Al K-edge spectra were collected in the total electron yield mode. All Al K-edge spectra were calibrated with metallic Al foil at the Al K-edge standard photon energy value.

1.2.2. Sample Preparation. — The samples were ground down to a micrometre size. To achieve an optimum signal-to-noise ratio, the transmission measurement with synchrotron radiation requires a sample thickness (x) given by $\mu x \approx 1$ where μ is the absorption coefficient; x was calculated assuming a Victoreen function for μ and gave $x \approx 15$ μm. The weighed amount of powder required to obtain the thickness was suspended in cyclohexane and then consolidated into a thin layer by drawing the solvent through a polycarbonate filter disc.

For the total electron yield mode (Al K-edge) samples were powdered and pressed onto copper slides with an intermediate indium foil to improve the contact between the powder and the copper sheet.

2. Results and Discussion

2.1. Data Reduction. — Conventional treatment was used to extract the EXAFS portion of the X-ray absorption spectrum [3]. The EXAFS function $\chi(k)$ obtained was k^2 weighted and Fourier transformed using a Kaiser-Bessel window function. This gave the radial distribution function of back-scattering atoms around the absorbing element. However, since the EXAFS phase shift function $\Phi_j(k)$ was carried over by the Fourier transformation, the Fourier transform peaks were shifted by 0.5 Å to lower distance. The contribution to the EXAFS spectrum of a particular shell was determined by Fourier filtering the corresponding peak (r_j) and back-transforming to k space. The back-transformed data were fitted using the program FITEX, which utilized the single scattering plane wave method to calculate EXAFS [3].

E_0, the photoelectron threshold energy, is generally believed to be in the vicinity of the edge. Unfortunately, there is no simple way to determine E_0 from the observed experimental spectrum: nor is there any universally characteristic of identifiable feature in the edge spectrum that will allow unequivocal determination of E_0. In the present case, the photo-electron threshold energy E_0 was initially assumed to be 4038 eV for the Ca K-edge and 1559 eV for the Al K-edge, and allowed to be refined in the fit. As will be detailed later, the spectra recorded at the Ca K-edge could be fitted using phase shift and backscattering amplitude derived from Mc Kale calculations [4], but these values were not suitable to fit the Al K-edge spectra. The mean free path of the photo-electron $\lambda(k)$, resulting from all the inelastic processes, was considered to vary with k as $\lambda(k) = k/(L/2)$ where L was a constant. The linear dependance of the electron mean-free path is a rough approximation, but it yields values which are in the expected

Table I. — *EXAFS radial distribution function for C_3AH_6 compared to XRD data.*

XRD (from Weiss *et al.* [5])			EXAFS (the present study)		
atom type	coordination number	shell radius (Å)	shell radius (Å)	L	dE_0 (eV)
O(I)	4	2.48	2.47	1 58	-13.4
O(II)	4	2.52	2.54	1.58	-13.4
Al(III)	4	3.51	3.52	1.52	-7.1
Ca(IV)	4	3.85	-	-	-
O(V)	8	4.00	-	-	-

range of magnitude. A parameter Q was used to measure the quality of the fit between the experimental and calculated EXAFS spectra.

The different parameters of the fit were (1) the distance r_j between the shell and the central atom, (2) the number N_j and type of atom in each shell, (3) the mean free path $\lambda(k)$ of the photo-electron, (4) dE_0, the shift in energy from the absorption edge, and (5) the thermal and structural disorder described by a Debye-Waller term $e^{-2k^2\sigma_j^2}$, where σ_j^2 was the sum of a thermal factor and the mean square deplacement between the central and neighbouring atoms $\left(\sigma_j^2 = \sigma_{j,\text{therm}}^2 + \sigma_{j,\text{struc}}^2\right)$. Only the structural term contributed to the Debye-Waller factor since the experiments were performed at low temperature.

The spectra recorded at the Al K-edge showed a large damping of the EXAFS modulations; information was then limited to the first coordination shell.

2.2. C_3AH_6

2.2.1. Structure of C_3AH_6. — C_3AH_6 is the only thermodynamically stable hydrate formed in calcium aluminate cements. Even if hydration at low temperatures gives rise to CAH_{10} or C_2AH_8, these metastable hydrates convert progressively to C_3AH_6 with time, and more rapidly when the temperature is raised or when they are stored under moist atmosphere. For this reason only the structure of C_3AH_6, which belongs to the garnet family, was resolved. It consists in a 3D framework built of $[Al(OH)_6]^{3-}$ non-shared octahedra, with Ca^{2+} ions occupying 8-coordinate positions in the interstices of the framework; hydrogen bonds slightly distort the $[Al(OH)_6]^{3-}$ octahedra and the dodecahedra $[Ca(OH)_8]^{6-}$ present two distinct Ca-O distances.

2.2.2. The EXAFS Spectrum of C_3AH_6. — The calcium environment in hydrogarnet C_3AH_6 was described as a series of shells. Values of the coordination number N_j and radius r_j, for each shell were calculated from the crystal structure of C_3AH_6 [5] and are listed in Table I. Experimental and theoretical EXAFS spectra of C_3AH_6 are compared in Figure 1a; the moduli of their Fourier transforms are presented in Figure 1b. Table I shows that r_j values did not have to be varied by more than a few picometres from those determined by X-ray crystallography.

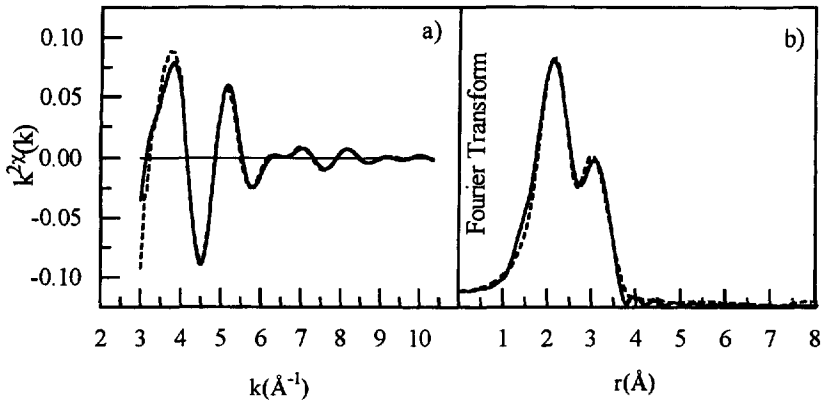

Fig. 1. — Experimental (full line) and theoretical (broken line) EXAFS spectra a), and Fourier transforms b) of C_3AH_6.

However, the shells Ca(IV) and O(V) refine to unreasonably large values of σ_j ($2\sigma_j^2 = 8 \times 10^{-2}$ Å^2). This suggested that their position could not be well defined by the EXAFS spectrum. This phenomenon was previously noted by Martens [6] when studying $CaCO_3$, for which the peaks related to C(II) and O(III) were missing in the radial distribution function around Ca. The authors demonstrated that nearly complete destructive interference of the O and C shell contributions was occuring, leading to the observed contradiction between EXAFS results and crystallographic data. In our case, the same phenomenon happens between the Ca(IV) and O(V) atoms. The total backscattering amplitudes for the two shells were calculated from Martens [6] as $A = (N/r^2)F \exp(-2r/\lambda)$, where N is the coordination number, r the distance, λ the mean free path of the photo-electron ($\lambda \approx 5$ Å) and F a parameter describing the backscattering power of the different neighbours. Values of F were estimated from Teo and Lee functions [7] and normalized to the backscattering power of O: 1, 1.7 and 2.3 were assigned to O, Al and Ca respectively. The calculation showed that the total backscattering amplitudes A of the two shells were nearly equal. Furthermore, the difference $\Delta\Phi$ of the total phase shifts between Ca(IV) and O(V) is given by:

$$\Delta\Phi = \Phi_{Ca} - \Phi_0 = (2kr_{Ca} + 2\alpha_{Ca} + \delta_{Ca}) - (2kr_0 + 2\alpha_{Ca} + \delta_0) = 2k(r_{Ca} - r_0) + \delta_{Ca} - \delta_0,$$

where α_{Ca} is the central atom phase shift, δ_{Ca} and δ_0 the phase shifts for the calcium and oxygen neighbours respectively. The phase shifts are calculated from Mc Kale results. In the EXAFS region of interest ($3 < k < 10$ Å^{-1}) the phase difference $\Delta\Phi$ is about π. Hence, identical backscattering amplitudes for the two shells, combined with a phase difference of π cancel the information about these two shells in the EXAFS spectrum, which explains the difficulty encountered when trying to fit them. This observation accounts for the large Debye-Waller factor of the Ca(IV) and O(V) shells. The destructive interferences between the Ca(IV) and O(V) shells are illustrated in Figure 2 by comparing their partial EXAFS spectra.

2.3. C_2AH_8

2.3.1. XRD Study. — Many doubts subsist concerning the structure of C_2AH_8. This hydrate forms hexagonal or pseudo-hexagonal plates with excellent (0001) cleavage, as do C_4AH_n and the numerous basic salts, all belonging to the so-called AFm phases. AFm phases have a layer structure derived from that of CH by the ordered replacement of one Ca^{2+} ion in three by

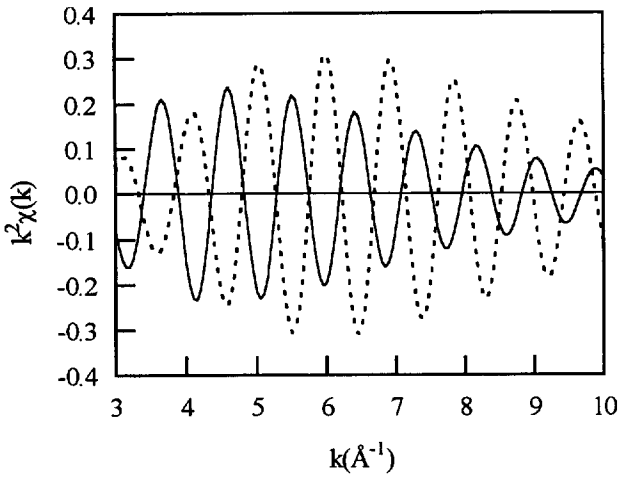

Fig. 2. — Destructive interferences between the Ca(IV) (dotted line) and O(V) (full line) shells.

Al^{3+} The principal layers thus defined alternate with interlayer containing anions such as OH^-, Cl^-, CO_3^{2-}, SO_4^{2-} and water molecules. The layer thickness depends on the nature of the anions and the amount of interlayer water. The C_2A hydrates are AFm phases with aluminium-containing species in the interlayer.

C_2AH_8 is the hydrate formed in metastable equilibrium with aqueous solution at 18 °C. Scheller *et al.* showed that the two phases α-C_2AH_8 and β-C_2AH_8 are not polymorphs of the same compound as previously proposed, but slightly differ in their water content: water content of 8 H_2O for the $\ll$ α-form $\gg$ and of 7.5 H_2O for the $\ll$ β-form $\gg$ were measured [8]. The hydrate investigated in this paper was then β-C_2AH_8. Taylor first described β-C_2AH_8 as an hexagonal cell with $a = 5.7$ Å and $c = 10.4$ Å [1]. β-C_2AH_8 was next investigated by Scheller *et al.* [8] who proposed a monoclinic cell with the parameters: $a = 9.93$ Å, $b = 5.74$ Å, $c = 42.2$ Å and $\beta = 97°$. An X-ray structure determination on the lower hydrate C_2AH_5 (which does not contain any water molecule in the interlayer) showed that this has the constitution $[Ca_2Al(OH)_6]^+[Al(OH)_4]^-$ [8]. There is still a disagreement about the coordination of the interlayer aluminium in C_2AH_8. Dosch *et al.* [9] suggested a tetrahedral coordination for this cation; however, a ^{27}Al NMR study of C_2AH_8 [10] indicated that the aluminium solely existed in octahedral coordination.

Lattice constant measurements were performed from X-ray diffraction powder patterns, using the program U_FIT [11]; Si was used as the internal standard (99.9%, PROLABO, $a = 5.43088$ Å). 18 lines of the powder diffraction diagram could be indexed on the basis of a monoclinic unit cell with the following parameters: $a = 9.946$ Å, $\beta = 5.733$ Å, $c = 43.138$ Å and $\beta = 97.96°$.

2.3.2. Al XANES of β-C_2AH_8. — The Al XANES spectrum of β-C_2AH_8 presented in Figure 3 consists of three main resonances; the feature located on the low energy side of the absorption edge (1565.4 eV) has a weak intensity. The absorption structure at 1567.7 eV corresponds to the 1s to 3p transition [12]; the component at 1571.5 eV, which is the most intense, has been related to resonances due to single and multiple scattering from shells beyond the first coordination shell of Al. Previously reported XANES spectra showed that Al K-edge spectroscopy can differenciate tetrahedrally from octahedrally coordinated aluminium; indeed, both calculated

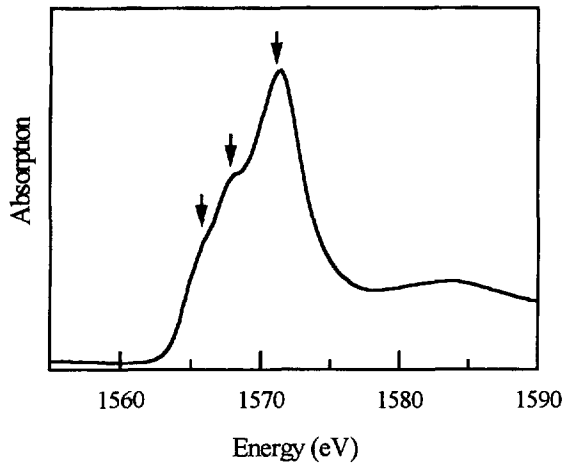

Fig. 3. — Al K XANES of C_2AH_8 (the arrows indicate the features determined by the derivative spectrum).

[13] and experimental [14] XANES spectra of Al^4 showed a strong single edge maximum at 1566 eV whereas Al^6 yields two distinct maxima at 1568 and 1572 eV, and a weak pre-edge feature at about 1566 eV. However, the overlap of the low pre-edge feature for the Al^6 and the absorption feature for Al^4 in the Al K XANES spectra causes a difficulty in estimating the Al^4/Al^{tot} ratio.

2.3.3. ^{27}*Al NMR and IR Study of* β*-*C_2AH_8. — The ^{27}Al CP-MAS NMR spectrum of the dicalcium aluminate hydrate consists of a sharp peak at 12 ppm and a broad peak between 40 and 80 ppm. The peak at 12 ppm was related to an octahedrally coordinated aluminium; the broad peak between 40 and 80 ppm indicated the presence of distorted $[Al(OH)_4]^-$ tetrahedra, which differs from the spectrum previously reported by Gessner *et al.* [10] who observed solely octahedrally coordinated aluminium in C_2AH_8. The Al^4/Al^{tot} ratio was estimated to be 50% [15].

On the IR spectrum, features related to the Al-O vibrations were located at 526 cm^{-1} and 865 cm^{-1}, according to previous studies on calcium aluminate hydrates [16]. The former absorption, common to all hydrates spectra, is assigned to octahedrally coordinated aluminium; only the C_2AH_8 IR spectrum exhibits the latter absorption, which is assigned to tetrahedrally coordinated aluminium [17] in agreement with the ^{27}Al NMR results.

2.3.4. EXAFS Spectrum of β*-*C_2AH_8. — In order to study the EXAFS spectrum of β-C_2AH_8, the distances around Ca were calculated from the crystal structure proposed for the AFm phases: C_2AH_5 [8] and C_4AH_{13} [18]. Distances in the principal layer were the same in both cases (we consider that the water molecule or hydroxyle ion which augments the coordination of calcium to seven belongs to the principal layer). Moreover, the shortest distances between Ca and an atom belonging to the interlayer was found to be 4 Å in C_2AH_5 (Ca-Al) and 4.2 Å in C_4AH_{13} (Ca-O). In the experimental radial distribution function, peaks appearing at distances lower than 4 Å would therefore be related to contributions from atoms located in the principal layer. The fit related to the two first peaks of the radial distribution function was performed by constraining dE_0 and λ (constant L) to the values refined for model compounds and by fixing N_j at the crystallographic value obtained from C_2AH_5; r_j and σ_j were allowed to vary

Table II. — *Comparison of calcium environment in C_2AH_5 as determined by X-ray diffraction and in C_2AH_8 as determined by EXAFS.*

XRD (from Scheller *et al.*[8])			EXAFS (the present study)		
atom type	coordination number	shell radius (Å)	shell radius (Å)	L	dE_0 (eV)
O(I)	6	2.39	2.41	1.5	-13.1
O(II)	1	2 55	2.56	1.5	-13.1
Al(III)	3	3.36	3.38	1.3	-7.5
Ca(IV)	3	3.50	3.52	1.2	-6.11
Ca(V)	6	5.73	5.74	1.4	-5.5
Al(VI)	-	-	5.23	1.3	-6.3

to provide the best agreement between theory and experiment. Table II compares the final values of the fit with the starting values calculated from the known crystal structure of C_2AH_5; the two sets of radii agree to within 1%. The fit of the fourth peak of the Fourier transform needs to be detailed. Distances calculated from the crystal structure indicated that only Ca(V) was contributing to this peak, if we did not consider the oxygen atoms; this approximation was justified by the small backscattering amplitude of oxygen atoms compared to aluminium or calcium ones. Figure 4a compares the resulting theoretical EXAFS spectrum related to this shell with that obtained experimentally; Fourier transforms are presented in Figure 4b. It appears that the EXAFS spectrum can not be satisfactorily fitted when considering only the Ca(V) shell. Only oxygen atoms or interlayer aluminium atoms can account for this discrepancy, because the other aluminium or calcium atoms belonging to the principal layer do not yield any distance in this range. The addition of an oxygen shell, for which only λ and dE_0 are constrained does not improve the fit. On the other hand, when an aluminium shell is considered, the fit is greatly improved, as can be seen in Figure 4, and confirmed by a lower value for Q. The fit leads to the existence of two aluminium atoms at a distance of 5.2 Å from the central Ca atom.

2.3.5. A Structural Model for β-C_2AH_8. — The distances and number of neighbours refined from the EXAFS study at the Ca K-edge confirmed that β-C_2AH_8 is an AFm phase. Moreover, an interesting information about the interlayer aluminium was obtained: aluminium is located at a distance of 5.2 Å from an average calcium atom. ^{27}Al CP-MAS NMR showed that 50% of the aluminium cations are tetrahedrally coordinated. Now thermogravimetric measurements, chemical analysis and powder X-ray diffraction confirmed that the sample under investigation did not contain any anhydrous phase; then, tetrahedrally coordinated aluminium atoms were effectively present in β-C_2AH_8. In this hydrate, half the aluminium cations belong to the principal layer and are octahedrally coordinated, the other half belonging to the interlayer. This therefore leads to a tetrahedral coordination for the interlayer aluminium cations. It is then possible to propose a location for these tetrahedrally coordinated interlayer aluminium atoms, distant of 5.2 Å from calcium. Some of the hydroxyl anions are supposed to be arranged in six-membered rings at $z = 1/2$. The remaining hydroxyl ions and water molecules are located above and below these rings, as described in Figure 5. This arrangement defines tetrahedral cavities and distance evaluation shows that the $[Al(OH)_4]^-$ tetrahedron just fits the space defined above. If we assume that the calcium coordination is increased to seven by water molecules,

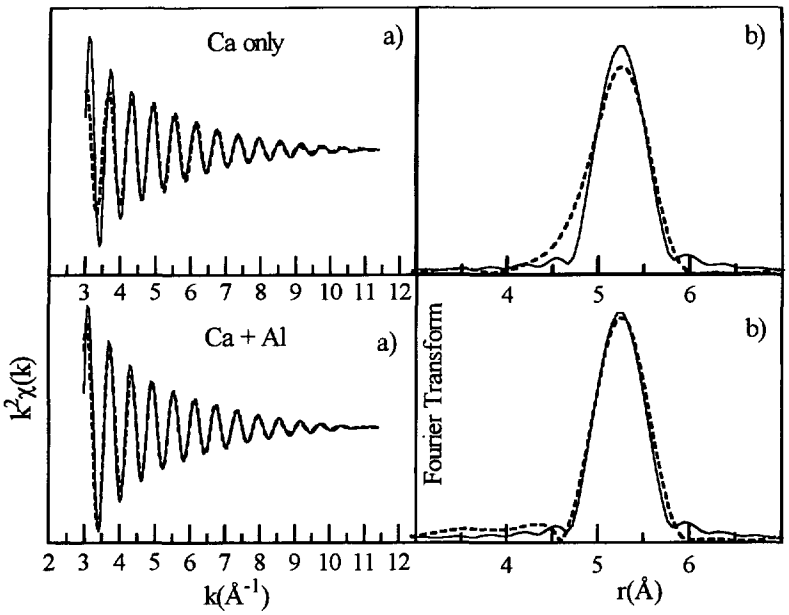

Fig. 4. — Experimental (full line) and theoretical (broken line) EXAFS spectra a), and Fourier transforms b), for the fourth peak of the radial distribution function of C_2AH_8. Fit with only Ca (top views) and with both Ca and Al (bottom views).

half the tetrahedral cavities are surrounded by hydroxyl anions alone, and the other half by three hydroxyl ions and one water molecule. Aluminium is therefore supposed to be located in the former cavities. This leads to three interlayer aluminium atoms located at 5.35 Å from calcium, as described in Figure 5. The distance that is calculated is in rather good agreement with that obtained by EXAFS measurements; calculation was done assuming a non-distorted tetrahedron, and a possible distortion could explain the small difference between calculated and experimental Ca-Al distances. However, the EXAFS refinement leads to two aluminium atoms at this distance, which is lower than the calculated number. As the aluminium atoms are rather distant from the calcium atom, other factors such as the Debye-Waller factor can modify the amplitude of the EXAFS signal; this could explain the discrepancy observed between the calculated and refined numbers of aluminium atoms.

2.4. CAH_{10}

2.4.1. XRD Study. — Monocalcium aluminate hydrate CAH_n is principally responsible for the hydraulic hardening of cement. As for the dicalcium aluminate hydrate C_2AH_n, it forms hydrates with a varying water content, the most hydrous member containing ten molecules of water. Many doubts subsist concerning the exact structure of CAH_{10}.

Buttler *et al.* gave tentative crystal data for CAH_{10} [19]: the crystals are hexagonal prisms, but not large enough for a single crystal XRD to be obtained, and attempts to determine the unit cell by electron diffraction failed due to loss of crystallinity in the instrument. The powder X-ray diffraction pattern was indexed on the basis of an hexagonal unit cell and the parameters obtained were: $a = 16.44$ Å, $c = 8.31$ Å; the unit cell contained 6 $[CAH_{10}]$. The authors suggested a constitution based on rings of six edge-sharing $[Al(OH)_6]^{3-}$ octahedra, similar to those that on further condensation yield the gibbsite structure.

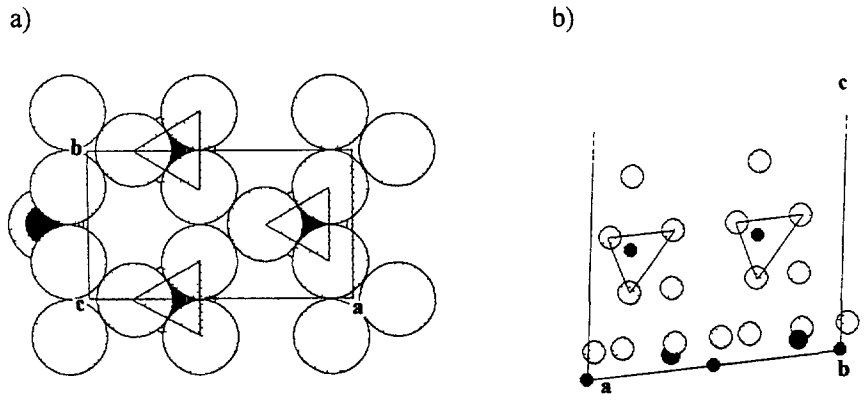

Fig. 5. — Description of the structure of C_2AH_8. a) Projection (001) of the interlayer content. (○): oxygen atoms, (•): aluminium atoms. b) Projection (010). (○): oxygen atoms, (•): aluminium atoms, (●): calcium atoms.

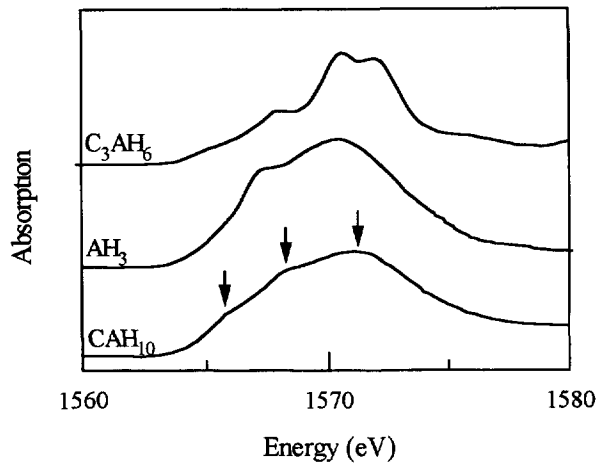

Fig. 6. — Al K XANES of CAH_{10}, AH_3 (from Ildefonse [14]) and C_3AH_6, showing the similarity between CAH_{10} and AH_3 spectra.

As previously mentioned, the composition of the monocalcium aluminate hydrate studied was $CAH_{9.4}$. 40 lines of the X-ray powder diffraction pattern were indexed assuming an hexagonal cell, and gave the following parameters: $a = 16.381$ Å, $c = 8.317$ Å.

2.4.2. Al XANES. — The Al K-XANES spectrum of CAH_{10} consists of three main resonances at 1565.8, 1568.1, and 1571.8 eV; the origin of these features were explained before. Figure 6 compares the Al K-XANES of CAH_{10} with that of other compounds containing octahedrally coordinated aluminium atoms. Al K-XANES spectroscopy is sensitive not only to Al coordination, but also to site symmetry, and number of sites [14]; the similarity between CAH_{10} and AH_3 XANES spectra then confirms the analogy between the structure of these two phases [19].

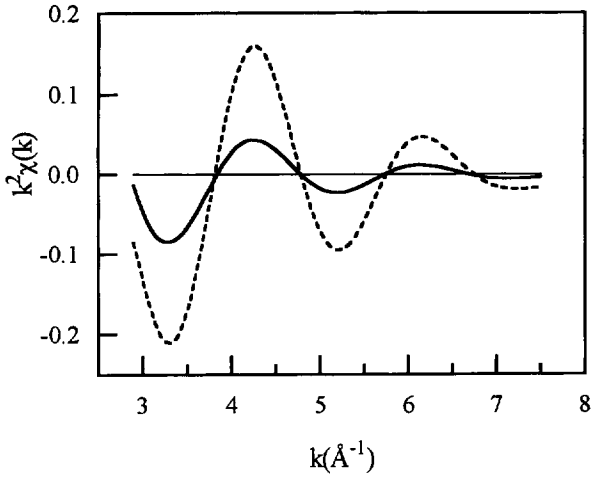

Fig. 7. — Al K-edge EXAFS contribution of the first oxygen shell in CAH_{10} (full line) and C_3AH_6 (broken line).

2.4.3. Ca K-edge and Al K-edge EXAFS Spectra of CAH_{10}. — Information on the local environment around calcium can be obtained from the EXAFS spectrum. The refinement related to the two first peaks of the radial distribution function gives six oxygen atoms at $r = 2.45$ Å ($\sigma = 0.08$ Å), and three aluminium atoms at $r = 3.42$ Å ($\sigma = 0.07$ Å).

The Al K-edge EXAFS spectrum of CAH_{10} also provides information on the environment around Al. Two difficulties were encountered when fitting Al K-edge spectra: Mc Kale calculations were not suitable to fit the EXAFS spectrum, and information was limited to the first coordination shell, due to a large damping of the experimental EXAFS oscillations. Then, the EXAFS contribution of the first oxygen shell is determined by Fourier filtering the corresponding peak (r) and back-transforming to the k space. The partial EXAFS spectrum was then compared to the spectrum of C_3AH_6, obtained with strictly the same procedure (type of window, window limits). The result is presented in Figure 7. As the central atom Al and the neighbouring atom O are identical in both cases, the phase shift $\Phi_j(k)$ is the same. The period of the signal $\chi(k)$ is then directly related to the Al-O distances and indicates a similar Al-O distance in both hydrates; this is in agreement with the ^{27}Al NMR results which show that, as in C_3AH_6, Al is merely octahedrally coordinated in CAH_{10}, leading to the same Al-O distance. However, the signal amplitude of $\chi_{CAH_{10}}(k)$ is dramatically reduced compared to $\chi_{C_3AH_6}(k)$; as Al coordination is the same in the two hydrates, only a higher Debye-Waller term in CAH_{10} can account for this difference. This assumption agrees with the close similarity between the structures of CAH_{10} and AH_3, $[Al(OH)_6]^{3-}$ octahedra being strongly distorted in the latter compound.

2.4.4. A Structural Model for CAH_{10}. — The complementary results obtained from XRD, ^{27}Al NMR and XAS allow us to propose a structural model for CAH_{10}. First, the given cell content and cell parameters, together with the analogy with the AH_3 structure indicate that CAH_{10} can contain two six-membered rings of $[Al(OH)_6]^{3-}$ edge-sharing octahedra in the hexagonal cell, which gives the formula $[Al_6(OH)_{24}]^{6-}$ for each ring. More, the powder diffraction pattern indexation indicates the extinction of the (001) line. Furthermore, XRD studies of the thermal behaviour of CAH_{10} reveal that the structure does not collapse when all the molecular water

Table III. — *Coordinates for the different atoms in the proposed structural model for* CAH_{10}.

atom type	x	y	z	atom type	x	y	z
Al(1)	0.1666	0.5000	0	OH(6)	0.1111	0.3888	0.8657
Al(2)	0.3333	0.5000	0	OH(7)	0.2777	0.5555	0.8657
Al(3)	0.5704	0.4296	0.5000	OH(8)	0.1111	0.7222	0.8657
Al(4)	0.7629	0.5258	0.5000	OH(9)	0.6666	0.2371	0.6343
Ca(1)	0.4500	0.5500	0.3700	OH(10)	0.7629	0.1409	0.6343
Ca(2)	0.5670	0.517	0.8700	OH(11)	0.8591	0.3333	0.6343
OH(1)	0.2222	0.6111	0.1343	OH(12)	0.5704	0.0446	0.6343
OH(2)	0.2222	0.4444	0.1343	OH(13)	0.6666	0.1409	0.3657
OH(3)	0.0555	0.4444	0.1343	OH(14)	0.8591	0.2371	0.3657
OH(4)	0.0555	0.6111	0.1343	OH(15)	0.7629	0.3333	0.3657
OH(5)	0.1111	0.5555	0.8657	OH(16)	0.4742	0.0446	0.3657

leaves the hydrate [19], leading to the formula $CaAl_2(OH)_8$; we therefore suppose that one ring $[Al_6(OH)_{24}]^{6-}$ is located at $z = 0$ and the other one at $z = 1/2$, with calcium ions linking the rings together. Positions for these six calcium ions have to be defined in such a way that the mean resulting calcium has three aluminium atoms at 3.4 Å. We consider that one of the rings is rotated through thirty degrees (360°/12) relative to the other one, to define a cavity surrounded by three aluminium atoms, in which calcium ions are located. The two calcium sites thus defined have three oxygen neighbours belonging to the $[Al(OH)_6]^{3-}$ octahedra. The octahedral coordination of Ca is achieved by some of the thirty-six water molecules that we have not considered in the model yet. These molecules can be arranged in six-membered rings, with a molecule above the center of each $[Al(OH)_6]^{3-}$ octahedron, which locates twelve molecules; the other twenty-four molecules can be situated in the holes of the framework, around z =1/4 and $z = 3/4$. Coordinates for calcium, aluminium and hydroxyl ions are listed in Table III and the structural model is described in Figure 8.

2.5. Dehydration of CAH_{10}. — The use of high-alumina cements for making refractory concretes involves heat treatments. One can distinguish three stages: i) at low temperatures ($T < 150$ °C), cementitious phases are hydrated, ii) at medium temperatures (150 °C < $T < 900$ °C), dehydration leads to amorphous or badly crystallized phases, with low cohesion, therefore, low mechanical properties, and iii) at high temperatures, ($T > 900$ °C), the sintering mechanisms lead to stable, oxydic phases, with high mechanical properties. An example of the loss in mechanical properties associated with dehydration is given in Figure 9, which shows that the dehydration of CAH_{10} results in a drop in Young's modulus of 80%.

2.5.1. XRD Study. — The dehydration of CAH_{10} gives rise to a continuous change in the X-ray powder pattern, marked by a decrease in cell parameters and changes in relative intensities [19]. Eventually, dehydration yields an amorphous material. CAH_{10} was heated to 90 °C, 150 °C, 300 °C, 800 °C and 930 °C. The XRD pattern of the 90 °C sample shows broadened peaks; by 150 °C, the sample appears to be completely amorphous. CA crystallized at 930 °C.

2.5.2. Al XANES. — The Al XANES spectra (Fig. 10) shows a significant progression with increasing temperature of the heat treatment. Especially evident is the development of the shoulder at 1565 eV, which corresponds to the tetrahedrally coordinated aluminium atoms. It must be reminded here that Al is tetrahedrally coordinated in the anhydrous phase CA but

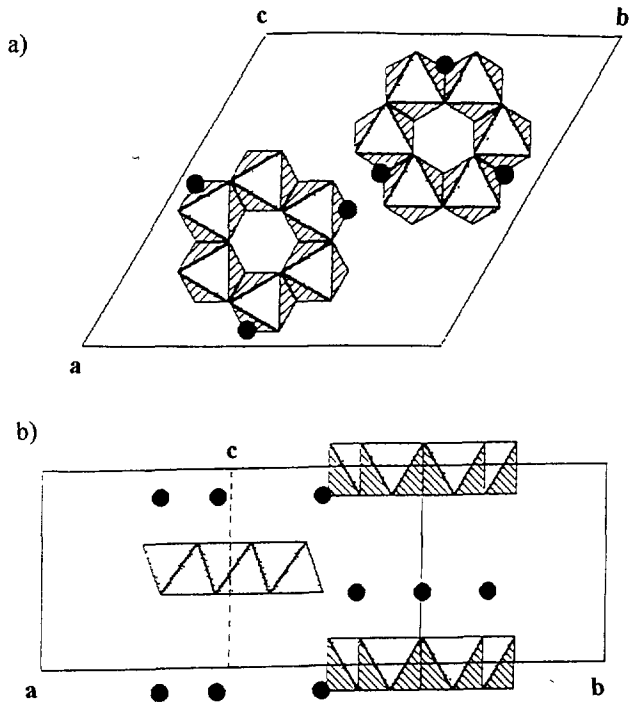

Fig. 8. — Description of the structural model proposed for CAH_{10}. (•): calcium atoms. a) Projection (001). b) Projection (100).

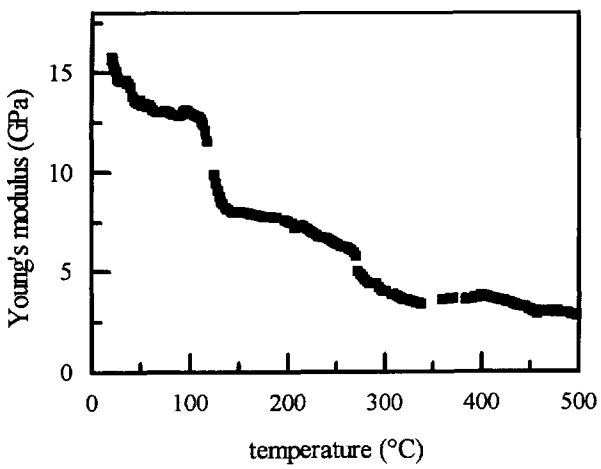

Fig. 9. — Young's modulus of CA hydrated at 4 °C, vs temperature.

it has a octahedral coordination in CAH_{10}. As previously mentioned, the estimation of the Al^4/Al^{tot} ratio is difficult, due to the overlap of the single feature of Al^4 and the pre-edge of Al^6. ^{27}Al MAS NMR is therefore under investigation to quantify the dehydration rate.

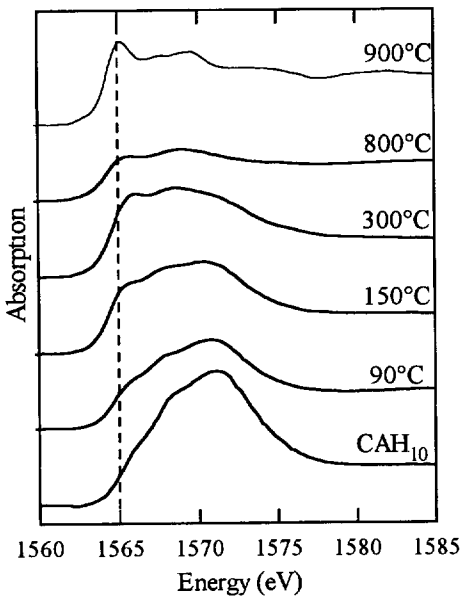

Fig. 10. — CAH_{10}: changes in the Al XANES spectrum vs heat treatment.

Table IV. — *Changes in the number of neighbours around calcium and distance Ca-O with heat treatment.*

temperature of heat treatment	distance Ca-O (Å)	number of neighbours	σ(Å)	X-ray diffraction results
15 °C	2.46	6	0.098	CAH_{10}
90 °C	2.45	5.5	0.099	$CAH_{n<10}$ poorly cristallized
150 °C	2.42	5.4	0.099	amorphous
300 °C	2.42	4 5	0.107	amorphous
800 °C	2.38 2.65	3 1	0.09 0.09	amorphous
930 °C	2.35 2.89	3.5 3.1	0.08 0.1	CA

2.5.3. Ca K-edge Spectra. — The analysis is limited to the first coordination shell. The same procedure (type of window, limits of the window...) is applied to extract the EXAFS oscillations from the experimental data whatever the temperature. As previously mentioned, the fit of the first oxygen shell in CAH_{10} leads to six atoms at a single distance 2.46 Å. CA is characterized by strongly distorted calcium sites: two oxygen shells distant from 0.54 Å (3.5 oxygen atoms at 2.35 Å and 3.1 oxygen atoms at 2.89 Å) are therefore considered when fitting the first peak of the radial distribution function of CA [20].

As the temperature of the heat treatment increases, the number of neighbours and the distance Ca-O decrease, as listed in Table IV.

Conclusion

C_2AH_8 is confirmed to be an AFm phase. We succeeded in localizing the tetrahedrally coordinated interlayer aluminium atoms.

Absorption experiments at the Al K-edge show a structural analogy between CAH_{10} and gibbsite (AH_3). A structural model for CAH_{10} is suggested, with locations for calcium, aluminium and hydroxyl ions. Dehydration of CAH_{10} leads to a decrease in the Ca-O distance and reduces the number of oxygen neighbours in the first coordination shell around Ca.

This study demonstrates that X-ray absorption spectroscopy is a powerful tool to characterize cementitious phases, with the particular advantage of being sensitive to the calcium environment.

References

[1] Taylor H.F.W., Cement Chemistry (Academic press 1968).

[2] Mangabhai R.J., Calcium Aluminate Cements (E. & F.N. Spon 1990).

[3] Bonnin D., Kaiser P. and Desbarres J., "Structures fines d'absorption des RX", Ecole CNRS (Garchy 1992).

[4] Mc Kale A. G., Veal B., Paulikas A. P., Chan S. K. and Knapp G. S., Improved *ab initio* calculation of amplitude and phase functions for extended X-ray absorption fine structure spectroscopy, *J. Am. Chem. Soc.* **110** (1988) 3763-3768.

[5] Weiss R. and Grandjean D., Structure de l'aluminate tricalcique hydraté, $3CaO.Al_2O_3.6H_2O$, *Acta Crys.* **17** (1964) 1329-1330.

[6] Martens G., Rabe P. and Wenck P., Destructive Interference and Multiple Scattering Effects Observed in Ca K-Edge EXAFS Spectra, *Phys. Stat. Sol.* **88** (1985) 103-111.

[7] Boon-Keng Teo and Lee P.A., *Ab initio* calculation of amplitude and phase functions for extended X-ray absorption fine structure spectroscopy, *J. Am. Chem. Soc.* **23** (1979) 2815-2832.

[8] Scheller Th. and Kuzel H.-J., "Studies on dicalcium aluminate hydrates", The 6th International Congress on the Chemistry of Cement (Moscow 1974) pp. 3-12.

[9] Dosch W., Keller H. and zur Strassen H., Proceedings of the 5th International Symposium on the Chemistry of Cement (1968) pp. 72-76.

[10] Gessner W., Müller D., Behrens H.-J. and Scheler G., Zur Koordination des Aluminiums in den Calciumaluminathydraten 2 CaO. Al_2O_3. $8H_2O$ und CaO. Al_2O_3. 10 H_2O, *Z. anorg. allg. Chem.* **486** (1982) 193-199.

[11] Evain M., "U-fit: A cell parameter refinement program", I.M.N. (Nantes, France, 1992).

[12] Mc Keown D.A., Waychunas G.A. and Brown G.E., EXAFS study of the coordination environment of aluminium in a series of silica-rich glasses and selected minerals within the Na_2O-Al_2O_3-SiO_2 system, *J. Non Cryst. Sol.* **74** (1985) 346-371.

[13] Mc Keown D.A., Aluminium X-Ray Absorption Near-Edge Spectra of Some Oxide Minerals: Calculation *Versus* Experimental Data, *Phys. Chem. Minerals* **16** (1989) 678-683.

[14] Ildefonse P., Calas G., Kirkpatrick R.J. and Montez B., "Local environment of aluminum in amorphous alumino-silicates by using XANES and MAS NMR.", Proceedings of the 7th International Symposium on Water-Rock Interaction (Utah 1992) pp. 153-158.

[15] Florian P., Department of Chemistry, The Ohio-State University (Private communication).

[16] Volant J., Etude par spectrométrie infrarouge d'aluminates de calcium hydratés, Thèse (Paris, 1966).

[17] Tarte P., Infra-red spectra of inorganic aluminates and characteristic vibrational frequencies of AlO_4 tetrahedra and AlO_6 octahedra, *Spectroch. Acta* **23A** (1967) 2127-2143.

[18] Ahmed S.J., Dent Glasser L.S. and Taylor H.F.W., Crystal Structures and Reactions of C_4AH_{12} and Derived Basic Salts, Proceedings of the 5th International Symposium on the Chemistry of Cement (1968) pp. 118-127.

[19] Buttler G. and Taylor H.F.W., Monocalcium aluminate decahydrate: unit cell and dehydration behaviour, *Il Cemento* (March, 1978) 147-152.

[20] Richard N., Lequeux N. and Boch P., An X-ray absorption study of phases formed in high alumina cements, to be published in *Adv. Cem. Res.*.